MEAN FLUXES OF SHORTWAVE RADIATION IN BROKEN CLOUDS

T.B. Zhuravleva, S.Yu. Popov, and G.A. Titov

Institute of Atmospheric Optics
Siberian Branch of the Russian Academy of Sciences, Tomsk
Received April 13, 1994

Influence of the random cloud field geometry upon mean upward and downward fluxes of shortwave solar radiation at different atmospheric levels is assessed. It is shown that relative differences in the mean fluxes at the cloud field boundaries between stratus and cumulus can reach tens of per cent; vertical profiles of radiative fluxes may qualitatively differ within clouds, depending on the underlying surface albedo value; and, absorption of the cloud layer due to aerosol particles, acting as condensation nuclei, strongly depends on cloud type and solar zenith angle.

1. INTRODUCTION

Among the constituents of codes of atmosphere general circulation models (GCMs) is the procedure for calculation of vertical profiles of upward and downward radiation fluxes which are needed to calculate radiant heat influxes. These latter radiative characteristics serve as an input ones for a number of atmospheric processes predicted with GCMs, e.g., the equation of radiant heat influx is sometimes a starting point to model formation and evolution of cloud fields, the equation of heat balance of the Earth's surface involves solar and thermal radiation fluxes that govern the surface thermal regime, and so forth. Since calculational errors can affect significantly the description of these processes, of importance is the question of accuracy of determination of the upward and downward radiation fluxes at different atmospheric levels.

Most of the present GCM codes make use of the models of plane–parallel, horizontally homogeneous atmosphere, and they are based computationally on the solution of the equation of radiative transfer using deterministic optical characteristics. In the case of partially overcast, influxes are calculateted as a linear combination of weighted influxes for the cases of clear and overcast sky, with weights depending on cloud fraction value. Such an approach is adequate only for the cases of stratus, when the parameter $\gamma \approx 0$ ($\gamma = H/D$, H is the cloud layer thickness, and D is the mean horizontal cloud size). Under the cumulus conditions ($\gamma \approx 1$), the approach can be regarded only as a first, fairly crude approximation[1,2] considering that the shortwave radiation transfer is affected remarkably by the stochastic geometry of cloud fields.

Mean albedo and transmission of shortwave radiation in the system "clouds–aerosol–underlying surface" are sufficiently investigated.[3,4] In the present work we raise the question about significance of the effect, the cloud field random geometry has on the mean upward and downward fluxes of the visible and near–IR solar radiation throughout the atmosphere. To this end, computations of the vertical profiles of radiant fluxes in cumulus are compared to those in equivalent (i.e., with the same optical characteristics) stratus. Treatment throughout the visible spectrum can be restricted to a discussion of results for a single wavelength, as the cloud optical characteristics change slightly, while the gas absorption is absent in this spectral range. In the near IR spectral range, mean fluxes are computed at once for a certain subinterval $\Delta\nu$ whose width is determined by the spectral resolution of exploited transmission functions of atmospheric gases (for our case $\Delta\nu \approx 10$–20 cm^{-1}).

2. MODEL OF ATMOSPHERE

Cloudy–aerosol atmosphere is considered as a set N_{lay} of homogeneous layers, each with constant atmospheric parameters inside. Clouds are normally separated as an individual layer with lower (bottom) H_{cl}^{b} and upper (top) H_{cl}^{t} boundaries; the upper and lower boundaries of the ith aerosol layer are designated as $H_{a,i}^{t}$ and $H_{a,i}^{b}$, respectively (Fig. 1). In dividing atmosphere, its layers should be chosen in accordance with those standard using in GCMs. Presently, there are many GCMs that differ, as an example, in their computational layering (e.g., see Refs. 5 and 6 and bibliography therein). For instance, the computation levels can be defined by the isobaric surfaces 1000, 850, 700, 500, 400, 300, 250, 200, 150, and 100 HPa. Realizing the impossibility of creating a universal radiation code which fits all of the existing GCM versions, we choose the levels enumerated above to divide the atmosphere. If necessary, computations can be performed for any isobaric surfaces prescribed. This remark also holds for transmission functions of atmospheric gases to be addressed below.
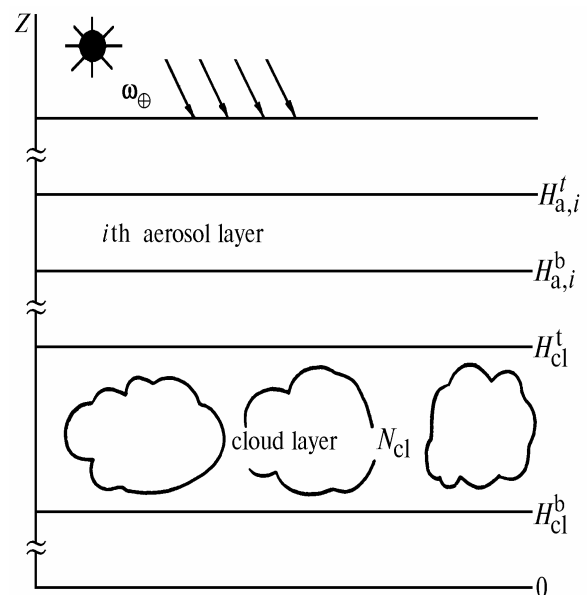

FIG. 1. Model of cloudy–aerosol atmosphere.

The vertical stratification and spectral behavior of aerosol extinction coefficient and single scattering albedo are chosen to correspond to the mean–cyclic model.[17] We chose to treat the absorption by water vapor and carbon dioxide with transmission function[8–10]

$$P_{\Delta\nu} = \exp\left(-\beta_\nu (w^*)^{m_\nu}\right)$$

with spectral resolution $\Delta\nu \approx 10\text{–}20$ cm^{-1}. Here w^* is the equivalent (reduced) absorber mass which for the plane–stratified atmosphere in a layer $\{z_1, z_2\}$ is defined by the formula

$$w^* = \frac{1}{\cos\theta} \int\limits_{z_1}^{z_2} \rho(z) \left(\frac{p(z)}{p_0}\right)^{n_\nu} dz \,,$$

where $\rho(z)$ and $p(z)$ are the absorber density and the pressure (in atm) at the altitude z, $p_0 = 1$ atm is the pressure at the altitude $z = 0$, and θ is the zenith viewing angle. We used in computations the altitude profile of water vapor for the midlatitude summer atmosphere.[11] Carbon dioxide was assumed to be uniformly mixed up to a 100 HPa altitude.

Clouds occupy the layer $1 \le z \le 1.5$ km. The broken cloud model and the Monte Carlo algorithm for calculating the mean upward and downward fluxes are given in Ref. 12 in detail. The underlying surface reflects according to the Lambert law. The radiant fluxes are given in relative units, as it is assumed that the top of the atmosphere is illuminated by a unit solar flux in direction $\omega_\otimes = (\xi_\otimes, \varphi_\otimes)$, where $\xi_\otimes$ and $\varphi_\otimes$ are the zenith and azimuthal solar angles, respectively (Fig. 1). Absolute values can be obtained by multiplying the results by $\pi S_\lambda \cos\xi_\otimes$, with the spectral solar constant πS_λ.

3. NUMERICAL RESULTS

The above– and under–cloud atmosphere are optically thin compared to clouds. So, in the absence of gas absorption, vertical profiles of fluxes outside the clouds will be practically the same as the mean fluxes on the cloud layer boundaries. Therefore, in this spectral interval, vertical profiles of the mean fluxes within the cloudy layer are of most interest. So, we confine ourselves to treating this atmospheric layer alone. Below, the results of computations at a wavelength $\lambda = 0.71$ μm are given, unless otherwise indicated.

Let $Q_{s,\mathrm{St}}(z)$ and $Q_{s,\mathrm{Cu}}(z)$ denote the mean downward fluxes, while $R_{\mathrm{St}}(z)$, $R_{\mathrm{Cu}}(z)$ are the mean upward fluxes of the scattered radiation in stratus and cumulus, respectively (brackets, meaning averages, are dropped for convenience).

At $A_s = 0$, for upward fluxes the inequalities hold: for $\xi_\otimes = 0°$ $R_{\mathrm{Cu}}(z) < R_{\mathrm{St}}(z)$, and for $\xi_\otimes = 60°$ $R_{\mathrm{Cu}}(z) > R_{\mathrm{St}}(z)$ (Fig. 2a). It is well known that in a deterministic scattering medium the flux of downward diffuse radiation has maximum for a certain optical depth. Analogous maximum is observed in the case of broken clouds (Fig. 2b). Differences between $Q_{s,\mathrm{St}}(z)$ and $Q_{s,\mathrm{Cu}}(z)$ are most dramatic at large values of $\xi_\otimes$. For $\xi_\otimes = 60°$, the maximum $Q_{s,\mathrm{Cu}}(z)$ sinks deeper from the upper cloud boundary and becomes flatter, as compared to the case of stratus. Differences in the mean fluxes of upward radiation between cumulus and equivalent stratus are caused by the effects associated with

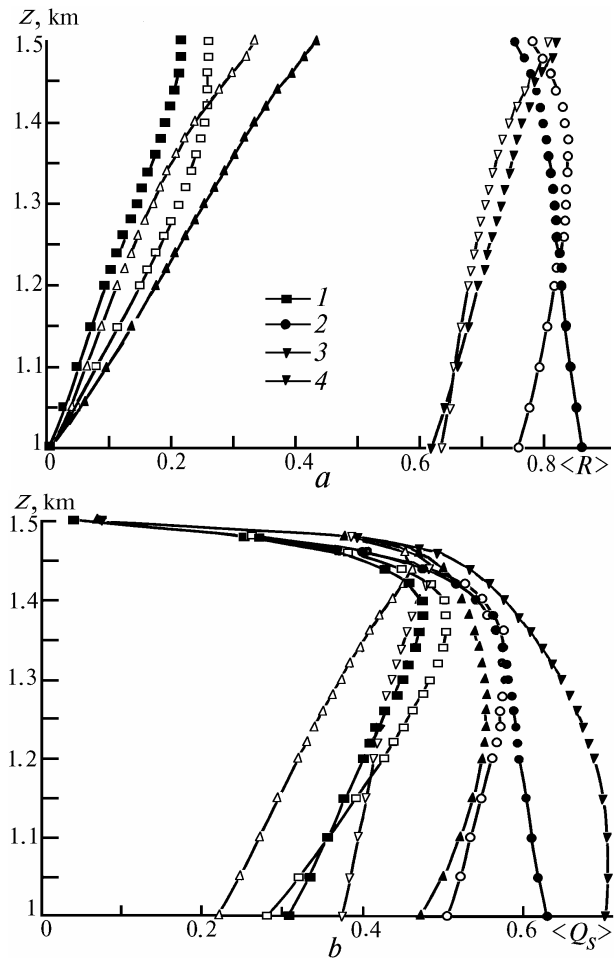the random geometry of cloud field and discussed in Ref. 2 in detail.

Fig. 2. Mean fluxes of upward (a) and downward (b) radiation at $\sigma = 30$ km^{-1}, $w_\lambda = 1$, $N = 0.5$, $D = 0.25$ km, and different values of solar zenith angle and underlying surface albedo: $\xi_\otimes = 0°$ (1 and 2), $\xi_\otimes = 60°$ (3 and 4), $A_s = 0$ (1 and 3), and $A_s = 0.8$ (2 and 4). Here and in Figs. 3, 4, and 6 closed symbols correspond to cumulus and open ones correspond to stratus.

Now we consider the influence of surface reflection ($A_s > 0$) on the vertical profiles of the mean fluxes. Surface–reflected radiation can be viewed as a diffuse source illuminating the bottom of atmosphere. Power and angle structure of radiation of this source depend upon the amount and angle structure of downward radiation at the surface level (plane $z = 0$), as well as upon the law of reflection from the surface.

Let $R_d(z)$ and $Q_d(z)$ denote the mean albedo and transmission of radiation from isotropic point source of unit power emitting into the upper hemisphere. Here and below, the subscript "d" stands for the corresponding flux calculated for such diffuse source. It is convenient to represent the solution of the problem in terms of the series of orders of reflection from the surface. Let $R^{(n)}(z)$ and $Q^{(n)}(z)$ denote contributions to the mean upward and downward fluxes from the nth reflection order, with $n = 1, 2 \dots$. It is obvious that

$$R^{(1)}(z) = A_s[S(0) + Q_s(0)]\, Q_d(z)\,,$$

$$Q^{(1)}(z) = A_s[S(0) + Q_s(0)]\, R_d(z)\,,$$

$$R^{(n)}(z) = A_s\, Q^{(n-1)}(0)\, Q_d(z)\,,$$

$$Q^{(n)}(z) = A_s\, Q^{(n-1)}(0)\, R_d(z)\,, \quad n = 2,\,\ldots\,,$$

where $S(z)$ is the mean flux of direct radiation for $A_s = 0$; $Q_d(z) = S_d(z) + Q_{s,d}(z)$. The fluxes $S_d(z)$, $Q_{s,d}(z)$, and $R_d(z)$ can be obtained by integrating, with known weight function, the fluxes S, Q_s, and R over solar zenith angle. The mean–value theorem dictates that $S_d(z)$, $Q_{s,d}(z)$, and $R_d(z)$ will be proportional to S, Q_s, and R calculated for certain intermediate values of solar zenith angle and for $A_s = 0$. Therefore, it can be expected that the

vertical profiles of $Q_{s,d}(z)$ and $R_d(z)$ will agree qualitatively with those of Q_s and R at $A_s = 0$. Obviously, $S_d(z)$ will be decreasing function of z.

Thus, for $A_s > 0$, a vertical profile of fluxes represents the sum of functions varying diversely and, perhaps, nonmonotonically with z. Hence, the profiles depend upon what summand dominates at a given z. This explains why the flux profiles for $A_s > 0$ may differ qualitatively from the corresponding profiles for $A_s = 0$ (Fig. 2).

Figure 2 illustrates flux computations in cumulus performed for $\gamma = 2$. This value of γ is close to a maximum one ever measured. So, it is believed that this figure gives maximum possible differences in radiation fluxes between cumulus and stratus. Obviously, with decrease of the parameter γ the difference decreases.
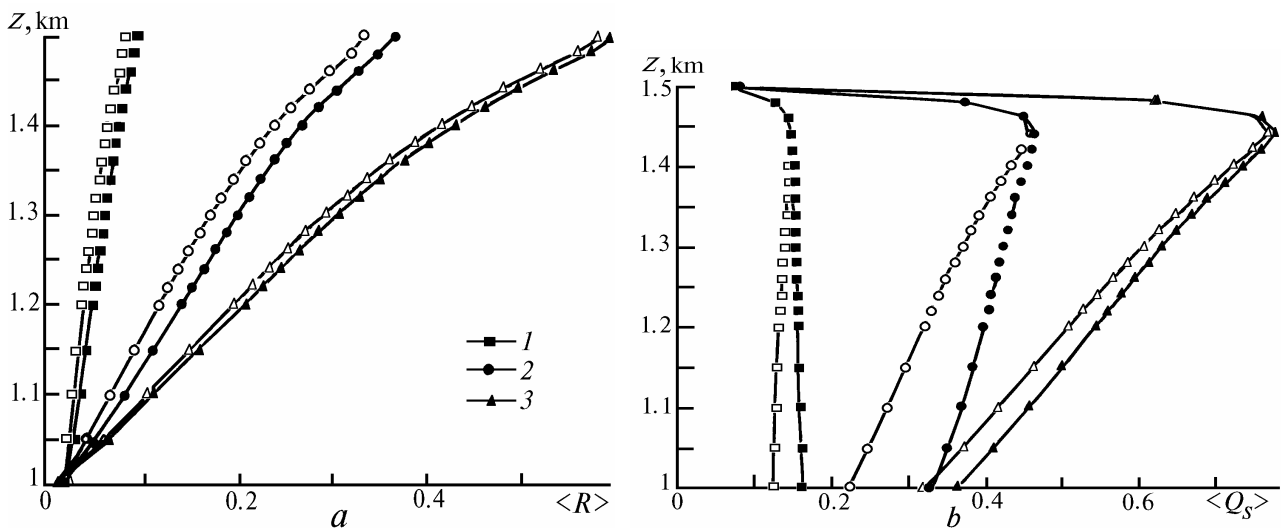

Fig. 3. Dependence of the mean fluxes of upward (a) and downward (b) radiation on cloud fraction at $\sigma = 30\ \text{км}^{-1}$, $w_\lambda = 1$, $D = 1$ km, $\xi_\otimes = 60°$, $A_s = 0$: $N = 0.1$ (1), $N = 0.5$ (2), and $N = 0.9$ (3)

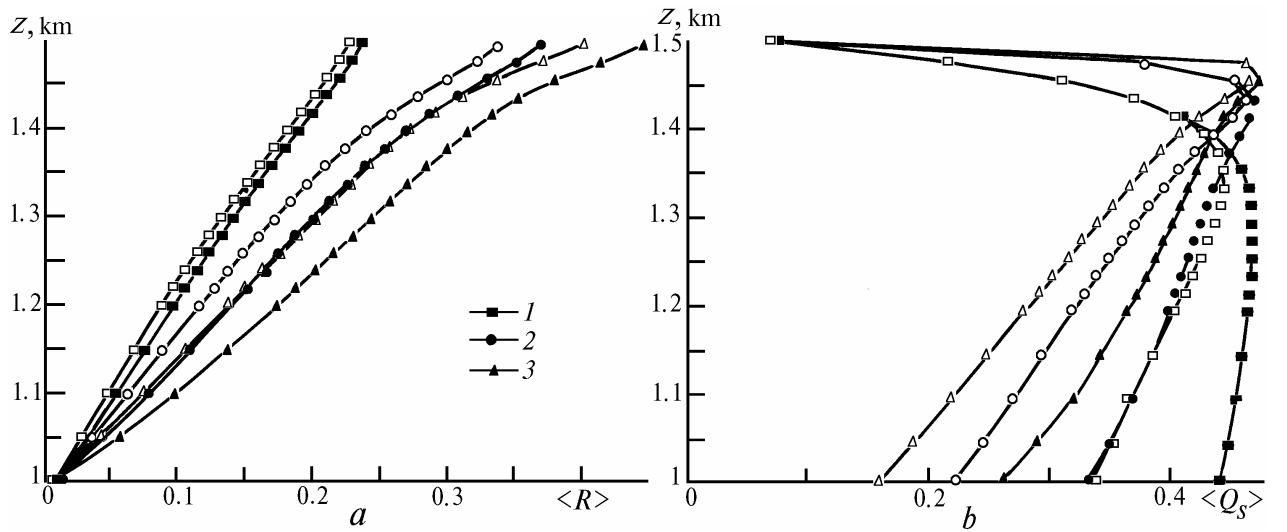

Fig. 4. Vertical profiles of upward (a) and downward (b) fluxes at $w_\lambda = 1$, $N = 0.5$; $D = 1$ km, $\xi_\otimes = 60°$, $A_s = 0$, and for different cloud extinction coefficients: $\sigma = 10$ (1), 30 (2), and 60 km^{-1} (3).

As expected, maximum differences between upward and downward radiation fluxes occur for intermediate cloud fractions (Fig. 3). At small N, downward radiation fluxes at first rapidly grow in the upper portion of cloud layer and then change little with decreasing altitude.

Dependence of the flux profiles upon cloud extinction coefficient is illustrated in Fig. 4. Note that a decrease in extinction coefficient is accompanied by readily explainable shift of the maximum of the downward radiation flux into the cloud layer interior.

It is commonly assumed that clouds scatter conservatively in the visible spectral range (i.e., the single scattering albedo $w_\lambda = 1$). However, aerosol particles, such as soot, present as condensation nuclei, can lower the value w_λ. Presence in clouds of even weak particulate absorption can significantly reduce (by tens of per cent) the mean albedo and transmission.[2] Now we consider the vertical profiles of the mean absorption inside the cloud layer.

We divide the cloud layer M into sublayers with boundaries z_i=const; $i = 1, ..., M$, $M + 1$; $z_1 = H_{cl}^b$, and $z_{M+1} = H_{cl}^t$. Let $P(z_i, z_{i+1})$ denote the mean absorption in a sublayer (z_i, z_{i+1}). Then $P(z_1, z_{M+1})$, or the mean absorption in the cloud layer, is defined as

$$P(z_1, z_{M+1}) = \sum_{i=1}^{M} P(z_i, z_{i+1}).$$

The relative absorption throughout a sublayer of thickness (z_i, z_{i+1}) is calculated as

$$p_i(z) = \frac{P(z_i, z_{i+1})}{(z_{i+1} - z_i)}.$$

In computations sublayers of variable thickness were used, namely: 0.05 km for altitudes from 1.0 to 1.2 km and 0.02 km for altitudes 1.2−1.5 km.

Obviously, for a given single scattering albedo, the absorption will grow with increasing fraction of diffuse radiation and the mean scattering order. For stratus, increasing the zenith solar angle reduces the absorption (Table I); this results from the growth of the albedo of cloud layer, and, perhaps, from possible decrease in the mean scattering order of reflected radiation due to strong forward elongation of the scattering phase function. This result is consistent with findings in Ref 13. For cumulus, the situation is quite the opposite because of a rapid growth of the fraction of diffuse radiation at large $\xi_\otimes$. For $\xi_\otimes = 0°$, the inequality $P_{St}(z_1, z_{M+1}) > P_{Cu}(z_1, z_{M+1})$ holds as caused by the fact that radiation exiting through the sides of cumulus has suffered on the average fewer scattering interactions. At $\xi_\otimes = 60°$, the effect associated with the increase, on the average, of the fraction of diffuse radiation dominates over that due to the decrease of the mean scattering order, so that the above inequality gets reversed.

TABLE I. The mean absorption in the cloud layer $P(z_1, z_{M+1})$ at $\sigma = 30$ km^{-1}, $D = 1$ km, $N = 0.5$ and $A_s = 0$.

w_λ	$\xi_\oplus = 0°$		$\xi_\oplus = 60°$	
	Stratus	Cumulus	Stratus	Cumulus
0.99	0.125	0.105	0.116	0.127
0.9	0.420	0.399	0.393	0.494

At $A_s = 0$, the histograms $p_i(z)$ have maxima located in the upper portion of the cloud layer whose positions and magnitudes depend upon cloud type (Fig. 5). The $p_i(z)$ and $Q(z)$ maxima are spatially correlated (see Fig. 2), so this portion of cloud layer can be thought of as a region of most intensive scattering. For large surface albedos, $p_i(z)$ increases most markedly in the lower and middle portions of cloud layer, thus reducing the lapse rates $p_i(z)$ when compared to the case of $A_s = 0$. This is due to diffuse radiation, which being reflected from the surface and scattered in the under−cloud atmosphere, illuminates the lower cloud boundary. As A_s grows, the histograms $p_{i, Cu}(z)$ increase faster than $p_{i, St}(z)$. This is attributed to the fact that the sides of numerous cumulus clouds act to reduce the mean flux of direct radiation of the above indicated diffuse source and, hence, to increase, on the average, the fraction of scattered radiation. We note that, for high values of A_s, the histograms $p_{i,Cu}(z)$ may have additional maxima in the lower portion of the cloud layer.

Let us discuss shortly the influence of the atmospheric gas absorption on the mean spectral fluxes of the near−IR solar radiation. Figure 6 illustrates profiles of the upward and downward radiation for wavelength $\lambda = 1.43$ μm at which the absorption due to water vapor and carbon dioxide takes place. The gas absorption produces an appreciable depletion of the upward and downward fluxes in the above−cloud atmosphere. Most strong atmospheric gas absorption occurs in the cloud layer in which the gases are assumed in sufficient concentrations, and the photon paths, due to multiple scattering, are substantially lenthened.
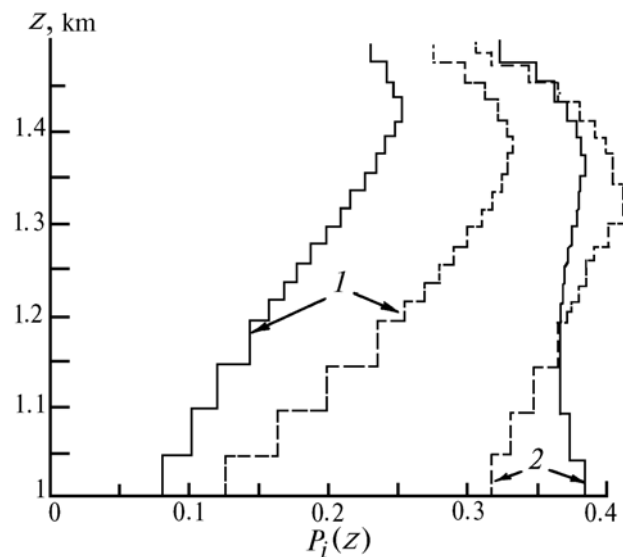

Fig. 5. Vertical profiles of absorption $p_i(z)$ at $\sigma = 30$ km^{-1}, $w_\lambda = 0.99$, $N = 0.5$, $D = 0.25$ km, $\xi_\otimes = 0°$, and for different surface albedos and cloud types: $A_s = 0$ (1) and $A_s = 0.8$ (2), cumulus (solid lines), and stratus (dashed lines).
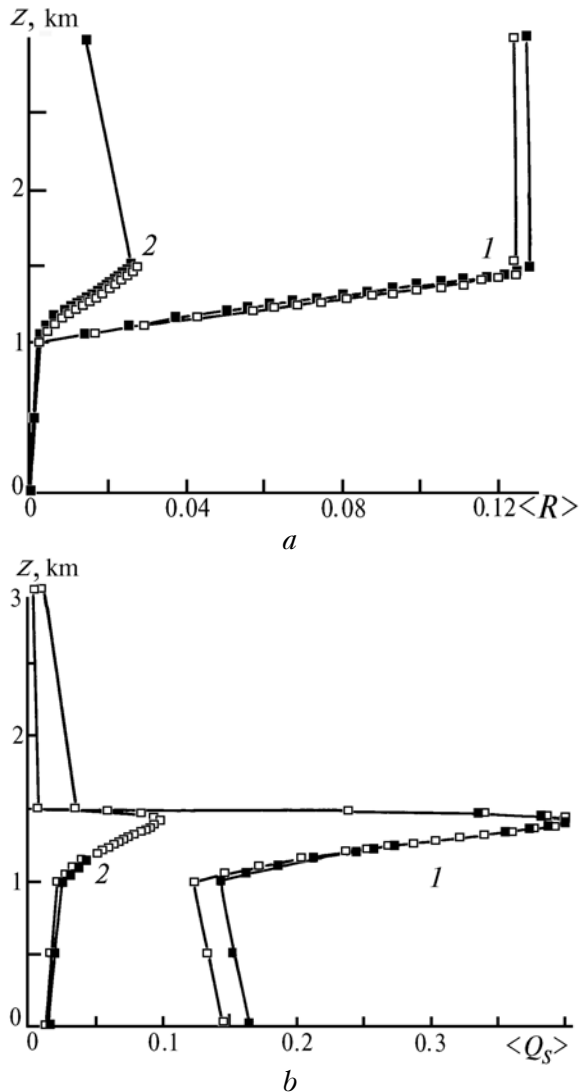
FIG. 6. Upward (a) and downward (b) radiative fluxes at a wavelength $\lambda = 1.43$ μm at $\sigma = 30.89$ km^{-1}, $w_\lambda = 0.967$, $N = 0.5$, $D = 1$ km, $\xi_\otimes = 0°$, and $A_s = 0$. Computations with (2) and without (1) regard to the absorption due to water vapor and carbon dioxide.

4. CONCLUSIONS

It is shown that at $A_s = 0$ upward fluxes may differ by as much as $\approx 20\%$ being computed at the upper boundaries of cumulus and stratus. Within the cloud layer, downward fluxes of diffuse solar radiation, as functions of altitude, may have maxima whose magnitudes and locations depend upon optical and geometrical parameters of cloud field and solar zenith angle. At $\xi_\otimes = 60°$, the downward flux of diffuse radiation at

a lower cloud boundary is nearly two times larger for cumulus than for stratus.

For $A_s > 0$, radiation reflected from the surface and scattered in the undercloud atmosphere plays a role of diffuse source illuminating cloud lower boundary and modifying boundary conditions. This is the reason for the vertical profiles of radiative fluxes to differ qualitatively from those in the case of $A_s = 0$.

Aerosol particles present in the cloud layer as condensation nuclei produce absorption that is essentially cloud−type−dependent. In particular, as the solar zenith angle increases from 0 to 60°, the absorption in stratus decreases, whereas in cumulus increases. Further, albedo of the underlying surface is an important parameter governing the distribution of absorption within the cloud layer. While for case of $A_s = 0$ the absorption is maximum in the upper portion of cloud layer, with large A_s a maximum absorption may occur in the vicinity of the cloud lower boundary.

REFERENCES

1. V.N. Skorinov and G.A. Titov, Izv. Akad. Nauk SSSR, Fiz. Atmos. Okeana **20**, No. 3, 263−270 (1984).
2. G.A. Titov, Izv. Akad. Nauk SSSR, Fiz. Atmos. Okeana **23**, No. 8, 851−858 (1987).
3. G.A. Titov, "Statistical description of the optical radiative transfer in clouds", Doctor's Dissertation in Physical and Mathematical Sciences, Tomsk (1989).
4. T.B. Zhuravleva, "Statistical characteristics of solar radiation in broken clouds". Candidate's Dissertation in Physical and Mathematical Sciences, Tomsk (1993).
5. R.G. Ellingson, J. Ellis, and S. Fels, J. Geophys. Res. **96 (D5)**, 8929−8954 (1991).
6. Y. Fouquart, B. Bonnel, and V. Ramaswamy, J. Geophys. Res. **96 (D5)**, 8955−8968 (1991).
7. V.E. Zuev and G.M. Krekov, Optical Models of the Atmosphere (Gidrometeoizdat, Leningrad, 1986), 256 pp.
8. B.M. Golubitskii and N.I. Moskalenko, Izv. Akad. Nauk USSR, Fiz. Atmos. Okeana **4**, No. 3, 346−359 (1968).
9. N.I. Moskalenko, Izv. Akad. Nauk SSSR, FAO Phys **5**, No. 11, 1179−1190 (1969).
10. V.A. Filippov, Izv. Akad. Nauk SSSR, Fiz. Atmos. Okeana **9**, No. 7, 774−775 (1973).
11. V.E. Zuev and V.S. Komarov, Statistical Models of Temperature and Gas Constituents of the Atmosphere (Gidrometeoizdat, Leningrad, 1986), 264 pp.
12. G.A. Titov, T.B. Zhuravleva, and V.E. Zuev, Mean Radiation Fluxes in the Near IR Spectral Range: Algorithms for Calculation (1994) [to be printed].
13. R. Davies, W.L. Ridgway, and K.−E. Kim, J. Atmos. Sci. **41**, No. 13, 2126−2137 (1984).